NJC

Accepted Manuscript

This is an *Accepted Manuscript*, which has been through the Royal Society of Chemistry peer review process and has been accepted for publication.

Accepted Manuscripts are published online shortly after acceptance, before technical editing, formatting and proof reading. Using this free service, authors can make their results available to the community, in citable form, before we publish the edited article. We will replace this *Accepted Manuscript* with the edited and formatted *Advance Article* as soon as it is available.

You can find more information about *Accepted Manuscripts* in the Information for Authors.

Please note that technical editing may introduce minor changes to the text and/or graphics, which may alter content. The journal's standard Terms & Conditions and the Ethical guidelines still apply. In no event shall the Royal Society of Chemistry be held responsible for any errors or omissions in this *Accepted Manuscript* or any consequences arising from the use of any information it contains.

ROYAL SOCIETY OF CHEMISTRY

www.rsc.org/njc

Graphical Abstract

The synthesis and the interaction between water soluble, non-aggregated, hexadeca substituted phthalocyanine zinc(II) pc with DNA and BSA was reported.

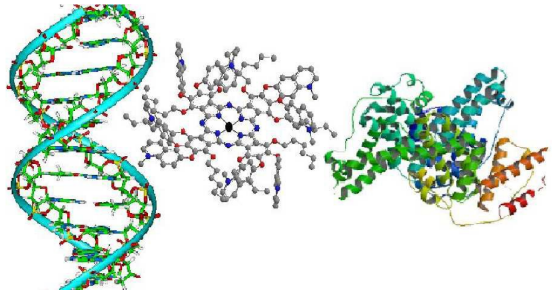

New Journal of Chemistry

ARTICLE

The synthesis and investigation of binding properties of a new water soluble hexadeca zinc(II) phthalocyanine with bovine serum albumin and DNA

Received 00th January 20xx,
Accepted 00th January 20xx

DOI: 10.1039/x0xx00000x

www.rsc.org/

Özge Kurt,[a] İbrahim Özçeşmeci,[a] B. Şebnem Sesalan,[a] M. Burkut Koçak*[a]

The synthesis and biological properties of a novel, hexadeca substituted zinc phthalocyanine (**3**) bearing 6-quinolinoxy units on the periphery together with hexyloxy chains on the non-periphery and its quaternized derivative (**3Q**) have been reported. The new quinolinoxy substituted zinc phthalocyanine (**3**) was synthesized and quaternized with the excess of methyl iodide to obtain the compound **3Q**. The binding of quaternized **3Q** with calf thymus DNA was investigated by UV–Vis and fluorescence spectrophotometric methods. The quenching effect of quaternized phthalocyanine on the fluorescence intensity of SYBR Gold –DNA complex was determined. The interaction between **3Q** and bovine serum albumin was investigated. The quenching effect of **3Q** on the fluorescence of Acridine Orange-BSA complex was determined. The results indicated that this water soluble zinc phthalocyanine can be used for biological and medicinal applications.

Introduction

Phthalocyanines (Pcs) are remarkable macrocyclic compounds having magnificent physical and chemical properties [1]. Recently, the application of Pcs in biology has increased due to their interesting properties. Pcs are particularly attractive since the macrocycle can be substituted by anionic or cationic groups such as carboxylic acid, sulfonic acid or quaternized amino groups [2-6] rendering them water solubility which is essential for PDT and catalysis in biological systems.

As the major soluble protein constituents of the circulatory system, serum albumins play an important role in the transport of many drugs [7-9]. BSA; as a protein model, is beneficial for investigation of drugs. Recently the synthesis of new metal complexes has become an important approach in different fields of chemistry, biology and bioinorganic chemistry [10].

The development of nucleic acid targeting drugs are very powerful means in the search for new potent drugs. Although many synthetic compounds have been developed to explore a variety of DNA/RNA structures, few molecules can be used to photocleave DNA in the concept of oncology such as photodynamic therapy (PDT) [11]. The reaction of metal complexes with DNA have been focused for a long time and the scope of synthesis of new reagents was to be beneficial for biotechnology and medicine [12].

A particularly attractive feature of Pcs is the possibility of tuning its electrical, optical, catalytic and photochemical properties through slight changes on the nature of the peripheral substituents or using different central metal ions in the Pc core [13-17].

Although the synthesis of tetra- and octa-substituted phthalocyanine derivatives has attracted a great deal of interest, hexadeca-substituted phthalocyanines are relatively less studied [18-20]. Therefore, recently we focus on synthesizing and examining the properties of hexadeca-substituted phthalocyanines [21-23]. Substitution of Pc macrocycle with electron donating groups cause bathochromic shift on the Q band absorption of Pc [18]. When identical substituents are compared, substitutions on non-peripheral positions cause larger shifts to longer wavelengths than peripheral positions [24]. Naturally, hexadeca-substituted Pcs with the electron donating groups on non-peripheral and peripheral positions are expected to shift larger wavelengths. This red shift is fruitful to do a research on biological activities especially for PDT applications.

In this work, the novel quinolinoxy substituted zinc Pc was synthesized, quaternized and the interactions of this compound (Scheme 1) with BSA and DNA were investigated.

[a]*Istanbul Technical University, Faculty of Science and Letters, Department of Chemistry, Maslak 34469, Istanbul, Turkey*
DOI: 10.1039/x0xx00000x

The binding modes of Pc to BSA and quenching effect of it on SYBR and AO was evaluated by UV–Vis and fluorescence titration experiments.

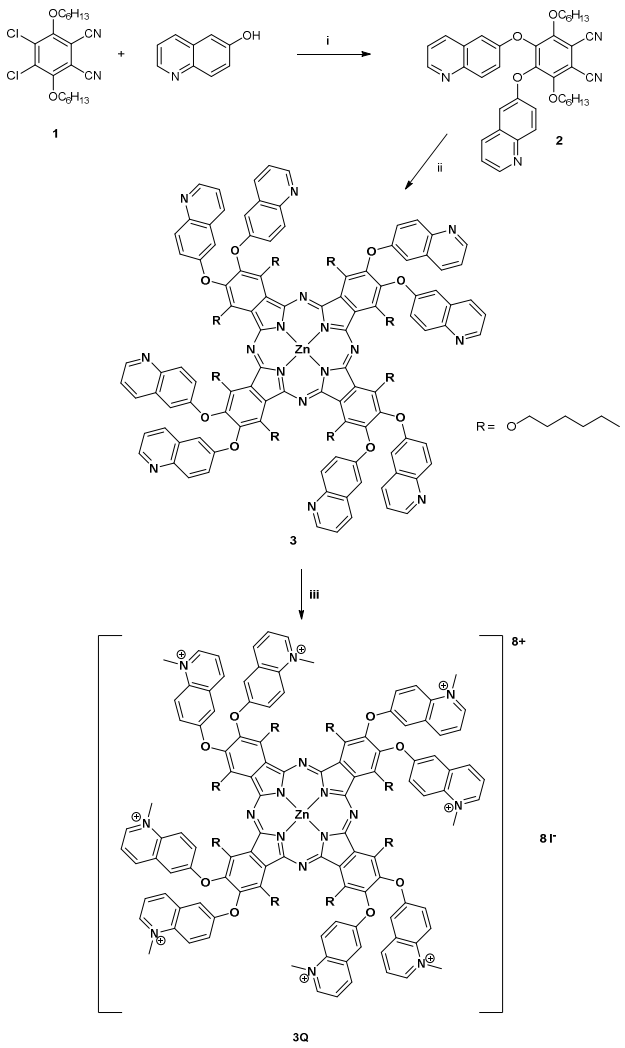

Scheme 1 The synthesis of ZnPc (**3**) and quaternized ZnPc (**3Q**)**.** (i): DMF, K_2CO_3, 110 ^oC, 6 h. (ii): n-hexanol, $Zn(CH_3COO)_2$, 160 ^oC, MW, 15 min. (iii): $CHCl_3$, excess MeI, RT, at dark, 7 days.

Results and discussion

Synthesis and characterization

Scheme 1 showed the synthetic route of hexadeca-substituted amphiphilic zinc phthalocyanine. The synthesis of a new phthalocyanine precursor bearing hexyloxy and quinolinoxy substituents was achieved by base-catalyzed nucleophilic aromatic displacement of 4,5-dichloro-3,6-bis(hexyloxy)phthalonitrile (**1**) with 6-hydroxyquinoline. The reactions were carried out at 110 ^oC under N_2 atmosphere for 6 h. The symmetrically hexadeca-substituted zinc phthalocyanine (**3**) was prepared in n-hexanol by template cyclotetramerization of **2** with anhydrous $Zn(CH_3COO)_2$ and a N-donor base DBU at 160 ^oC in a sealed tube under microwave irradiation for 15 min. The crude product was purified by chromatography using 1:5 ethyl acetate:n-hexane then with ethylacetate as the eluent on silica-gel filled column. Water- soluble zinc phthalocyanine (**3Q**) were obtained from the reaction of zinc phthalocyanine with the excess of methyl iodide in $CHCl_3$ at room temperature for 7 days [25]. The analyses of the newly synthesized compounds were consistent with the predicted structures as shown in the experimental section. The complexes were characterized with spectroscopic techniques such as the UV-Vis, FT-IR, NMR spectra and mass spectroscopy.

In the FT-IR spectra for phthalonitrile (**2**), we clearly saw the aromatic -CH vibrations at 3058 cm^{-1}, the aliphatic -CH vibrations at 2954, 2928, 2859 cm^{-1} and the sharp peak due to C≡N vibrations at 2233 cm^{-1}. Cyclotetramerization of the dinitrile derivative to zinc Pc (**3**) was confirmed by the disappearance of the C≡N vibration which was attributed to **2**. No major change was found in the IR spectra of **3Q** after quaternization.

MALDI-TOF MS spectra of compound **2** showed $[M+H]^+$ peak at 615.549. Phthalocyanine complex **3** showed $[M+3H]^+$ peak at 2525.49 and $[M+2H+DHB]^+$ peak at 2678.59.

The ^1H NMR spectrum of **2** in DMSO-d_6 indicated aromatic protons at 8.72 ppm as a doublet of doublets, at 8.11 and 7.87 ppm as doublets, and 7.42-7.38 as multiplets with a total integration of 12 protons. Ar-O-CH_2 protons of hexyloxy group were observed as triplet at 4.15 ppm. The CH_2 protons of hexyloxy group resonated between 1.46 and 0.97 ppm as multiplets. For the terminal methyl protons of the side chains were observed as a triplet at 0.63 ppm. The difference between the ^1H NMR spectra of **2** and **3** was the broad signals due to the aggregation of planar phthalocyanine molecules at high concentrations generally used for NMR measurements. In ^1H NMR spectrum of **3Q**, quaternization of quinolinoxy moieties by methyl iodide results an electron withdrawing structure so that aromatic protons shift at downfield area when compared with **3** [26]. The aromatic protons of **3Q** resonated between 9.33 and 8.03 ppm, whereas aromatic protons of **3** resonated between 8.73 and 7.23 ppm. One additional signal for N^+-CH_3 protons were observed at 4.57 ppm as singlet.

Electronic absorption studies and aggregation behaviors

Naturally, these hexadeca-substituted phthalocyanine complexes with substituents on both non-peripheral and peripheral positions with electron-donating groups produced larger bathocromic shifts [27].

Thanks to its great solubility, we have been able to investigate ZnPc's UV-vis absorption characteristics in ranging from non polar to polar solvents. Q band absorption of ZnPc **3** in different solvents such as toluene, diethylether, dichloromethane, THF, chloroform, ethylacetate, acetone, and pyridine was given in Fig. 1. The Q band absorption changed around 727-739 nm depending on solvent. In general, the red shift of the Q band increased with the ascending

refractive index of the solvent. Additionally, compound **3** exhibited a new red-shifted absorption band in chloroform and dichloromethane (Fig. 1). It was suggested that the observed new red-shifted absorption band occurred due to the protonation of the meso-nitrogens in the phthalocyanine core. It was most likely caused by acidic impurities in various solvents (chloroform, dichloromethane, benzene, n-hexane) to J type aggregation[21, 28]. Addition of 30 µL pyridine to **3** in dichloromethane converts the spectrum back to original form by descending in the protonated band at 800 nm and ascending in the Q band (see inset in Fig.1).

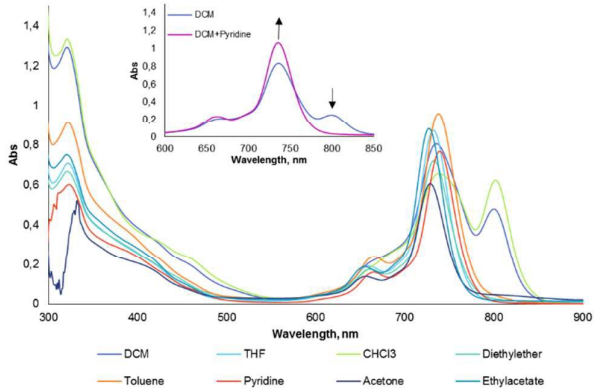

Figure 1 Absorption spectra of ZnPc (**3**) in different solvents at same concentration ($6x10^{-6}$ M) (inset: deprotaned Q band in violet line and protonated Q band in blue line).

The concentration dependence of the UV-Vis spectra of zinc **3** and quaternized zinc **3Q** phthlocyanines was further assessed in order to prove the absence of aggregation [29]. So, in this study, we investigated the aggregation behaviour of the zinc phthalocyanine **3** at different concentrations in THF (Fig. 2) and quaternized ZnPc **3Q** in water (Fig. 3). As the concentration was increased, the intensity of the absorption of the Q band also increased and there were no new bands (normally blue shifted) due to the aggregated species [21, 30].

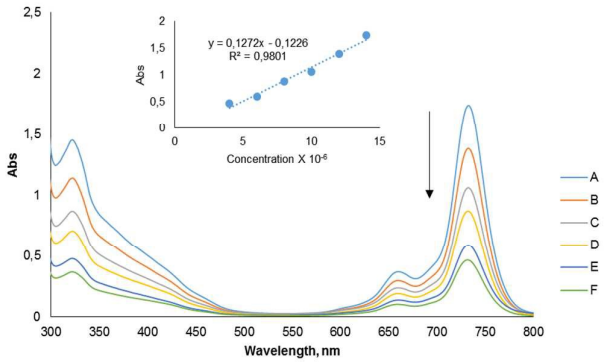

Figure 2 Absorption spectra of ZnPc (**3**) in THF at different concentrations: $1.4x10^{-5}$ M (A), $1.2x10^{-5}$ M (B), $1.0x10^{-5}$ M (C), $8x10^{-6}$ M (D), $6x10^{-6}$ M (E) and $4x10^{-6}$ M (F).

Table 1 Photophysical parameters of **3** in THF and **3Q** in aqueous media.

	B band	log ε	Q band	log ε	Excitation	Emission	Stokes	Φ_F

In the electronic spectra of the zinc phthalocyanines **3** and **3Q**, B bands were observed at 322 and 321 nm. Their intense Q bands appeared at 732 and 720 nm with weak vibronic absorptions at 660 and 656 nm, respectively (Fig.2, Fig.3, Table 1).

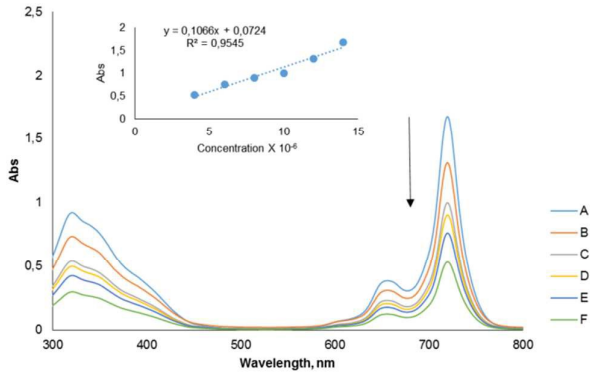

Figure 3 Absorption spectra of quaternized ZnPc (**3Q**) in aqua at different concentrations: $1.4x10^{-5}$ M (A), $1.2x10^{-5}$ M (B), $1.0x10^{-5}$ M (C), $8x10^{-6}$ M (D), $6x10^{-6}$ M (E) and $4x10^{-6}$ M (F).

Fluorescence Spectra

The steady-state fluorescence spectra of **3** and **3Q** were performed in THF and water respectively, upon excitation at the 650 nm Q-band vibration for **3** and excitation at the 655 nm Q-band vibration for **3Q**. Emission aroud 741 nm for **3** and 750 nm for **3Q** (Fig. 4), occurred almost entirely from the phthalocyanine moiety (Table 1). Due to the hydrocarbon chains on non-peripheral positions, **3Q** has no aggregation in aqueous solutions so all fluorescence was observed in the absence of Triton-X-100. The Q band of hexadeca substituted phthalocyanine's luminescent spectra were red shifted when compared to the corresponding peripheral substituted phthalocyanine complexes. 40-60 nm bathochromic shifts in emission were observed in non-peripheral substituted phthalocyanine complexes when compared with peripheral substituted ones [22]. The excitation of **3** and **3Q** spectra were similar to absorption spectra and both were mirror images of the fluorescent spectra in solvents. The proximity of the wavelength of each component of the Q-band absorption to the Q-band maxima of the excitation spectra for ZnPc's suggested that the nuclear configurations of the ground and excited states were similar and are not affected by excitation in solvents. The observed Stokes shifts (Table 1) were typical of phthalocyanine complexes [31].

	λ max, (nm)		λ max, (nm)		λ Ex, (nm)	λ Em, (nm)	shift (nm)	
3	322	5.05	732	5.14	727	741	9	0.092
3Q	321	4.82	720	4.86	732	750	30	0.034

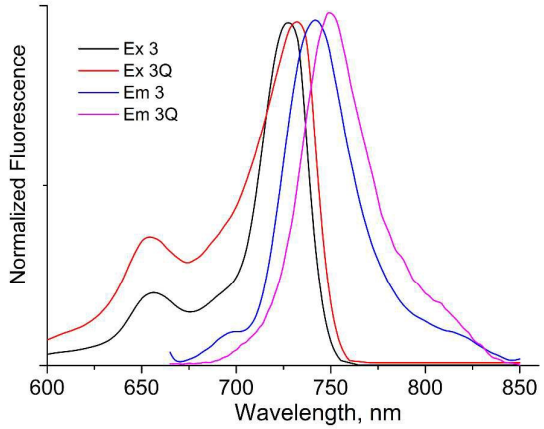

Figure 4 Excitation and emission spectra of 3 in THF and 3Q in water. Excitation wavelengths: 650 nm for **3** and 655 nm for **3Q**.

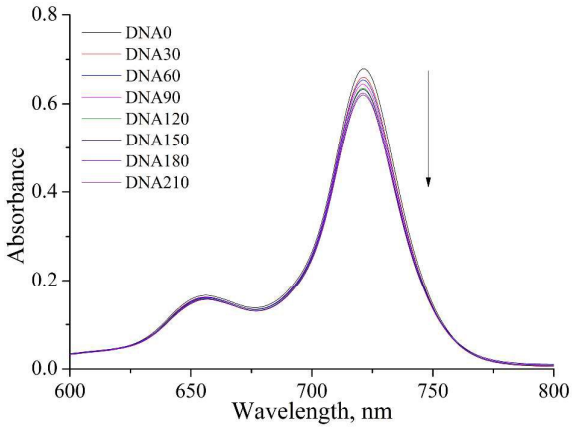

Figure 5 The spectral changes in UV-Vis absorption spectrum of **3Q** in aqueous media upon addition of DNA.

Fluorescence quantum yields (Φ_F) were determined by the comparative method (Eq. 1) [32]:

$$\Phi_F = \Phi_F(_{Std}) (FA_{Std}\eta^2 / F_{Std}A\eta^2_{Std}) \quad (1)$$

where F and F_{Std} are the areas under the fluorescence curves of phthalocyanines derivatives and the standard, respectively Octakis(hexylthio)phthalocyaninatozinc(II) was employed as a standard in DMSO (Φ_F = 0.10) [33]. Both the sample and the standard were excited at the same wavelength.

The fluorescence quantum yields (Φ_F) of **3** and **3Q** were given in Table 1. The measured fluorescence quantum yields for hexadeca-substituted phthalocyanines were much lower than unsubstituted ZnPc (Φ_F = 0.25) in THF [34] at room temperature. An apparent reason might be non-peripheral hexyloxy groups enhanced vibrational and rotational motion that may deactivate the excited states [18].

Interaction of 3Q with DNA

It was observed that as the interaction of Pc with DNA increased, maximum absorbances of Pc decreased. Purple lines in Fig. 5 (lines from 6 and 7 in Fig. 5 were running together which means after addition of 180.0 µL CT-DNA to **3Q** and the Q band absorbance remained constant) showed the end of titration which means maximum interaction between Pcs and DNA occurred. According to Fig.5, **3Q** displayed no shift at Q band (722 nm) and Soret band region. In case of **3Q**, the lack of shift in band maxima and a small hypocromicity of quaternized Pcs was consistent with electrostatic binding between positive Pc and negative phosphate backbone of DNA.

Assuming that the observed changes in fluorescence result from the strong interaction between the drug and DNA. Each run in Fig. 6. involved a different DNA concentration and binding constants were calculated according to the plot drawn Log [(F_0-F)/F] vs. Log [DNA] (inset in Fig. 6). The structure having both hydrophilic pyridinium moieties on peripheral and hydrophobic alkyl chains on non-peripheral positions of a Pc core had the great of interest and was the key to determine the binding mode of **3Q** with DNA according to the data given in Table 2. K_b values allowed interpreting that the substitution of small cationic units in **3Q** increased the affinity of the molecules towards DNA. The decrease in fluorescence intensity of **3Q** upon the addition of DNA was due to the formation of DNA-**3Q** complex. While pyridinium moieties on **3Q** could intercalate to DNA, hexyloxy chains force to change its conformation for an electrostatic attraction with phosphate groups. In other words, both hydrophilic and hyrophobic units on **3Q** compound ease the interaction with DNA. Furthermore, when the complex intercalates with DNA, the π*- orbital of the ligand (in this work **3Q**) can couple with the π orbital of the DNA base pairs and decrease the π*- π transition energy causing bathochromism. Finally, the coupling of π – π* orbital is partially filled by electrons, decrease the transition probabilities resulting in hypochromism [35]. The association binding constants calculated from Fig. 6. and given in Table 2 supported mainly an intercalative binding with DNA due to dominant effect of pyridinium moieties over alkyl chains [36, 37].

Table 2 K_b, K_{sv} and *n* values of **3Q** with standart deviations (± STD).

	K_b (x10^3)(L x mol^{-1})	K_{sv} (x10^3)(L x mol^{-1})	*n*
BSA	1.15 ± 0.6	101.02 ± 0.6	0.52 ± 0.2

DNA	39.81 ± 0.6	46.99 ± 0.6	0.9 ± 0.2

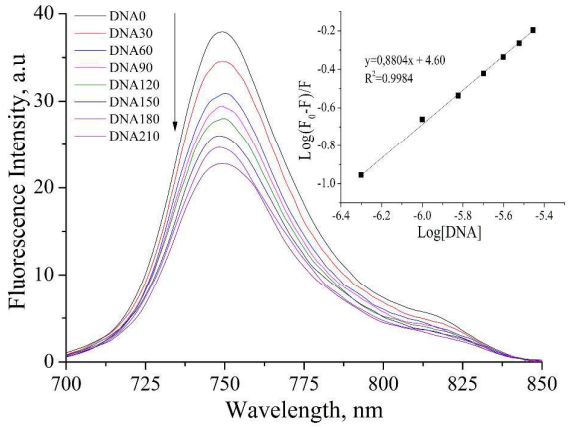

Figure 6 The spectral changes in fluorescence emission spectrum of **3Q** in aqueous media upon addition of DNA (inset: The plot for determination of K_b).

SYBR Gold is a known DNA stain used in biological applications and a greatly enhanced fluorescence at 527 nm is observed when bound to DNA [38]. Therefore, a competition of binding assay between SYBR and **3Q** could determinate the mode of interaction with DNA. The fluorescence of free SYBR-DNA complex was notably diminished by the strong fluorescence quenching effects of quaternized compounds. The quenching effect was determined by using Stern-Volmer K_{sv} constants (Table 2, Fig. 7). The K_{sv} value of **3Q** was indicating that the more pyridinium cationic units, the more intercalative binding affinity to DNA, the more quenching effect on fluorescence of SYBR-DNA complex [39]. The quenching depends on the formation of a stable Pc–DNA complex less fluorescent than free Pc. The least fluorescence was observed when the most stable Pc–DNA complex formed. This means that DNA preferred Pc instead of SYBR. Thus the decrease in fluorescence emission evidenced the existance of an effective interaction between Pcs and DNA. These results were in agreement with K_b values supporting an intercalation binding mode (Table 2, Fig.7).

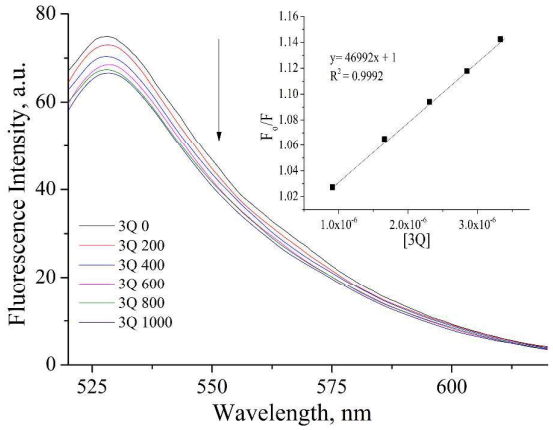

Figure 7 The spectral changes in fluorescence emission spectrum of SYBR-DNA in aqueous media upon addition of **3Q** (inset: The plot for determination of K_{sv}).

Interaction of 3Q with BSA

The complexes formed between BSA and 3Q upon the addition of BSA at different concentrations led changes both in absorption and fluorescence spectra. To follow the formation of BSA-Pc complex in UV–vis spectra, the decrease in absorbance, *c.a*. 7 nm red shift and when the complete neutralization occurred, the absorbance was fixed at a constant value (Fig. 8). Last lines in Fig. 8. mean that after addition of 180.0 µL BSA to 3Q, the Q band absorbance remained constant. They showed the end of titration which means maximum interaction between 3Q and BSA occurred. The bathochromic shift in the Q band position was observed on addition BSA, Fig. 8. This implies that a complex is actually being formed between the 3Q and albumin. The lack of broadening or splitting of Q band proved that upon interaction with BSA, 3Q is not aggregated [40]. It is indicated that when there was more interaction between Pc and BSA, the concentration of free-Pc was decreased and consequently absorbances were decreased.

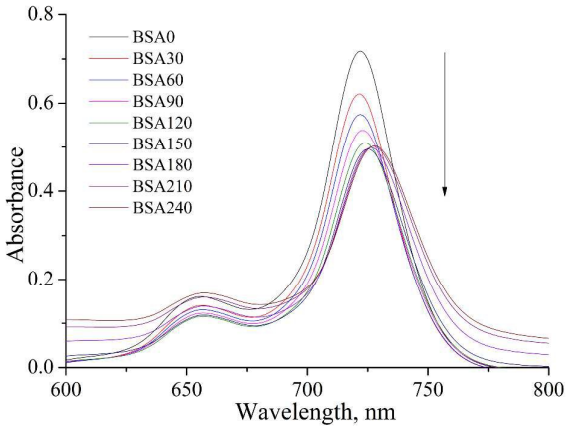

Figure 8 The spectral changes in UV-Vis absorption spectrum of **3Q** in aqueous media upon addition of BSA.

The fluorescence titration experiments of the compound **3Q** with BSA were shown in Fig. 9. BSA binding resulted in reasonable fluorescence quenching which is manifested in decrease in the fluorescence intensity. When BSA was successively added to the aqueous solution of Pc, the emission intensities of **3Q** decreased. In folded proteins the tryptophan (in BSA) emission is usually suppressed by the presence of charged residues [41]. The spectral changes in Fig. 9 implied that cationic pyridinium groups of **3Q** interact with negatively charged residues resulting a decrease in emission. Thus K_b value given in Table 2 proved that **3Q** was non-aggregated.

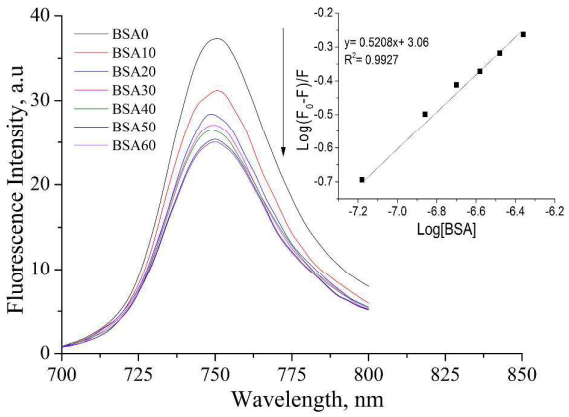

Figure 9 The spectral changes in fluorescence emission spectrum of **3Q** in aqueous media upon addition of BSA (inset: The plot for determination of K_b).

On the other hand, to prove the interaction of **3Q** with BSA, a known nucleic acid cationic dye; AO was used to determine whether BSA would prefer AO or **3Q**. AO has an enhanced fluorescence upon binding with BSA at 351 nm [42]. Therefore, a competition of binding assay between AO and **3Q** would determine the the quenching mechanism. The fluorescence of free BSA-AO complex was diminished by the strong fluorescence quenching effects of quaternized **3Q**. As seen in Fig. 10, when **3Q**, was bound to BSA tightly, characteristic BSA-AO flourescence decreased. Table 2 indicated that **3Q** had a strong quenching effect as result of charged units present both on DNA and **3Q** which are constructed by salt bridges. K_b and K_{sv} values given in Table 2 implied that statitic quenching mechanism proceded on non-aggregated **3Q** [40].

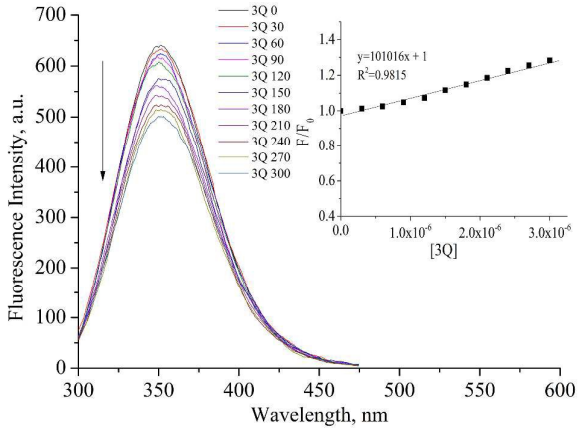

Figure 10 The spectral changes in fluorescence emission spectrum of AO-BSA in aqueous media upon addition of **3Q** (inset: The plot for determinate of K_{sv}).

Conclusions

In this work, a novel hexadeca substituted zinc phthalocyanine **3** was synthesised and quinolinoxy groups on the peripheral positions was quaternized with methyl iodide to obtain water soluble **3Q** derivative. Electronic absorption spectra and aggregation behaviour of the phthalocyanines were investigated. The synthesized phthalocyanine complexes show excellent solubility in polar and apolar solvents due to their amphiphilic nature. According to Beer-Lambert Law, no aggregation was observed for compound **3** in tetrahydrofuran in the concentration range from 4×10^{-6} to 1.4×10^{-5} M. Eventhough we did not add any ionic or non-ionic surfactants (*e.g.*Triton-X-100), quaternized zinc phthalocyanine **3Q** did not show aggregation on the range of 10^{-5}-10^{-6} M in water.

The main goal of the present study was to examine the interaction of DNA and bovine serum albumin with a chemical structure which has hydrophobic substituents together with hydrophilic moieties on phthalocyanine core. While pyridinium positively charged units intercalate, lipophilic hexyloxy groups on non-peripheral positions hindered aggregation.

On the other hand, proteins such as albumin has the ability to coordinate or to interact with cationic species. The experimental results proved that a stable bovine serum

albumin -**3Q** complex occured in aqueous media. The most important efficacy of all experiments was that **3Q** was monomeric (non-aggregated) possibly by the effect of hexyloxy groups on non-peripheral positions of phthalocyanine ring. Thus the chemical structure of the novel phthalocyanine (**3Q)** benefited to experience all biological assays in aqueous media without using agents such as Triton-X-100. According to Table 2 and figures (8-10), water-soluble quaternized zinc phthalocyanine (**3Q**) strongly bind to bovine serum albumin, thus being a model as drug vehicle in bood plasma. Future clinical success will proceed on photodynamic theraphy and genetics with interdisciplinary collaboration.

Experimental

Materials and equipments

IR spectra were recorded on a Perkin-Elmer Spectrum One FT-IR (ATR sampling accessory) spectrometer and electronic spectra on a Scinco S-3100 spectrophotometer using 1 cm path length cuvettes at room temperature. Proton nuclear magnetic resonance (^{1}H NMR) and carbon nuclear magnetic resonance (^{13}C NMR) spectra were recorded on Agilent VNMRS 500 MHz spectrometer using TMS as internal reference. Mass spectra were performed on a Bruker Microflex LT MALDI-TOF MS spectrometer. Single mode reactor (CEM DISCOVER SP) was used for microwave heating. Fluorescence excitation and emission spectra were measured by using Perkin-Elmer LS-55 fluorescence spectrophotometer. BSA (bovine serum albumin) and Acridine Orange (AO) were obtained from Aldrich. All solvents were dried and purified as described by Perrin and Armarego [43]. Anhydrous metal salts were finely ground and dried at 100 ^{o}C. The purity of the products was tested in each step by TLC (SiO_2). 4,5-dichloro-3,6-bis-(hexyloxy)phthalonitrile (**1**) was prepared according to reported procedures [18, 19].

Synthesis of compounds

Synthesis of 3,6-bis(hexyloxy)-4,5-bis(quinolin-6-yloxy)-phthalonitrile (2). 4,5-dichloro-3,6-bis-(hexyloxy)phthalonitrile (**1**) (1.2 g, 3 mmol) was dissolved in 10.0 mL dry DMF at room temparature and 6-hydroxyquinoline (1.75 g, 12 mmol) was added to this solution. After stirring for 15 min, 2.88 g of finely ground anhydrous K_2CO_3 (20 mmol) was added portion wise during 1 h with efficient stirring. The reaction mixture was stirred under nitrogen at 110 ºC for further 5 h. After being cooled to room temperature, the mixture was poured into ice/water (100 mL). The resulting deep brown solid was extracted with dichloromethane. The organic solution was dried with Na_2SO_4 and the solvent was evaporated to give the crude product. Finally pure product was obtained by column chromatography on silica gel with 1:1 THF:n-hexane. Yield: 0.958 g, 52%. mp 97-98 °C. UV-Vis ($CHCl_3$): λ_{max} nm (log ε) 246 (5.44), 321 (5.04). IR (ν, cm^{-1}): 3058 (Ar-H), 2928-2859 (CH, aliphatic), 2233 (C≡N), 1621 (Ar C=C), 1201 (Ar-O-Ar). ^{1}H NMR (500 MHz, DMSO-d_6): δ, ppm 8.72 (dd, 2H), 8.11 (d, 2H), 7.87 (d, 2H), 7.42-7.38 (m, 6H), 4.15 (t, 4H), 1.46 (p, 4H), 1.11 (p, 4H), 1.01-0.97 (m, 8H), 0.63 (t, 6H). ^{13}C NMR (126 MHz, DMSO-d_6): δ, ppm 153.90, 152.56, 149.24, 145.98, 144.50, 134.99, 130.79, 128.33, 121.86, 120.29, 113.30, 110.23, 106.37, 75.44, 30.39, 29.15, 24.59, 21.78, 13.61. MS (MALDI-TOF): m/z 615.549 $[M+H]^+$.

Synthesis of 1,4,8,11,15,18,22,25-octakishexyloxy-2,3,9,10,16,17,23,24-octakis(quinolin-6-yloxy)phthalocyaninato zinc(II) (3). A mixture of compound **2** (220 mg, 0.36 mmol), anhydrous metal salt $Zn(CH_3COO)_2$, (34 mg, 0.175 mmol) and catalytic amount of DBU (1,8-diazabicyclo[5.4.0]undec-7-ene) in 2.0 mL of n-hexanol was irradiated in a microwave oven at 160 ^{o}C, 200 W for 15 min. After cooling to room temperature the green suspension was precipitated with water-ice mixture, filtered, washed with the same solvent, and finally dried in vacuo. The purification of the crude product was accomplished by column chromatography on silica gel first with 1:5 ethyl acetate:n-hexane then with ethylacetate as the eluent. Yield: 32 mg, 15.5%. mp > 200 ^{o}C. UV-Vis (THF): λ_{max} nm (log ε) 322 (5.02), 660 (4.42), 732 (5.09). IR υ (cm^{-1}): 3059 (Ar-H), 2923-2854 (CH, aliphatic), 1622 (Ar C=C), 1213 (Ar-O-C). ^{1}H NMR (500 MHz, $CDCl_3$): δ, ppm 8.73 (b, 8H), 8.10-7.80 (m, 24H), 7.52 (b, 8H), 7.23 (b, 8H), 5.00 (b, 16H), 1.63 (b, 16H), 1.00-0.70 (m, 48H), 0.52 (b, 24H). ^{13}C NMR (126 MHz, $CDCl_3$): δ, ppm 156.25, 148.47, 144.78, 135.76, 134.73, 128.79, 125.50, 121.26, 120.94, 120.21, 109.79, 75.44, 31.42, 29.69, 25.65, 22.29, 13.77. MS (MALDI-TOF): m/z 2525.49 $[M+3H]^+$, 2678.59 $[M+2H+DHB]^+$.

Synthesis of 1,4,8,11,15,18,22,25-octakishexyloxy-2,3,9,10,16,17,23,24-octakis(1-methyl-quinolin-6-yloxy) phthalocyaninato zinc(II) octaiodide (3Q). Compound **3** (0.050 g, 0.02 mmol) was dissolved in chloroform (2.0 mL) and methyl iodide (0.114 g, 0.8 mmol) was added to this solution. The reaction mixture was kept for 7 days in dark. The resulting precipitate was filtered off, washed with chloroform, diethyl ether and then dried. Yield: 0.048 g, 65%. mp > 200 ^{o}C. UV-Vis (H_2O): λ_{max} nm (log ε) 321 (4.82), 656 (4.44), 720 (5.08). IR υ (cm^{-1}): 3031 (Ar–H), 2925–2855 (CH, aliphatic), 1624, 1595 (Ar C=C), 1261 (Ar-O-C). ^{1}H NMR (500 MHz, DMSO-d6): δ, ppm 9.33 (d, 8H), 9.04 (d, 8H), 8.50 (d, 8H), 8.25-8.03 (m, 24H), 4.92 (b, 16H), 4.57 (s, 24H), 1.49 (b, 16H), 1.21 (b, 16H), 0.86 (b, 16H), 0.70 (b, 16H), 0.48 (t, 24H). ^{13}C NMR (126 MHz, DMSO-d6): δ, ppm 159.72, 152.05, 149.07, 146.45, 142.58, 131.63, 128.90, 116.82, 116.27, 110.03, 76.65, 63.86, 46.32, 31.49, 29.99, 25.46, 22.36, 14.31, 8.56. MS (MALDI-TOF): m/z 3516.06 $[M\text{-}I\text{-}CH_3]^+$, 3358.33 $[M\text{-}I\text{-}CH_3\text{-}(C_{10}H_9NO)]^+$, 3199.00 $[M\text{-}I\text{-}CH_3\text{-}2(C_{10}H_9NO)]^+$.

Determination of binding of 3Q to CT-DNA using UV–Vis titrations

All titrations of Pc with CT-DNA were performed at room temperaturein distilled water. The concentrations of CT-DNA per nucleotide phosphate ([DNA]) was calculated from the absorbance at 260 nm using ε_{DNA} = 6600 M^{-1} cm^{-1} [44]. DNA was

stored at 4°C overnight and used within 2 days. 50.0 µM DNA and 10.0 µM **3Q** stock solutions were prepared in distilled water. 2 mL aqueous solution of **3Q** was placed in 3 mL quartz cuvette (a final concentration of 9.05 µM) and 7 x 30 µL injections of DNA were added manually. Absorption spectra were collected from 300 to 800 nm. The titrations were carried out until Q bands remain at a fixed wavelength upon the successive additions of CT-DNA.

Determination of binding of 3Q to BSA using UV–Vis titrations

All titrations of Pc with BSA were performed at room temperature in distilled water. 20.0 µM BSA and 10.0 µM **3Q** stock solutions were prepared in distilled water. 2 mL aqueous solution of **3Q** was placed in 3 mL quartz cuvette (a final concentration of 8.92 µM) and 8 x 30 µL injections of BSA were added manually. Absorption spectra were collected from 300 to 800 nm. The titrations were carried out until Q bands remain at a fixed wavelength upon the successive additions of CT-DNA.

Determination of binding 3Q to DNA using fluorescence measurements

The binding of water soluble complex **3Q** to DNA were studied by spectrofluorometry at room temperature. An aqueous solution of **3Q** (10.0 µM, 2.5 mL) was titrated by successive additions of 30.0 µL aliquots of 50.0 µM DNA. After each addition of DNA, the fluorescence emission spectra were recorded. The concentration of DNA along the titration varied from 0 to 3.87 µM. Fluorescence excitation and emission spectra were obtained from solutions of DNA and quaternized zinc Pc (**3Q**) were prepared in distilled water. Excitation and emission slits were set at 10 nm bandpass at 900 V. Pcs solutions were excited at 655 nm and spectra were recorded between 650 and 850 nm. The steady diminution in Pcs fluorescence with increase in DNA concentrations was noted and used in the determination of the binding constants and the number of binding sites on DNA, according to Eq. (3) [45].

$$nQ + B \leftrightarrow Qn + B \quad (2)$$

where B is biomolecule like Pc (unbound or free form), Qn is DNA with n binding sites. Here, Qn + B is the quenched biomolecule (Pc when bound to DNA) whose association constant is K_b.

$$K_b = [Qn + B]/([Q]^n [B]) \quad (3)$$

If the overall amount of Pc is B_0, then $[B_0] = [B] + [Qn + B]$. Here [B] is the concentration of the unbound Pc. According to this data, the relationship between the fluorescence and the unbound Pc can be defined as $[B]/[B_0] = F/F_0$ where F is the fluorescence of the unbound Pc during the addition of DNA and F_0 is the initial intensity of Pc

$$\log(F_0\text{-}F)/F = \log K_b + n\log[DNA] \quad (4)$$

where F_0 and F are the fluorescence intensities of Pc complex (**3Q**) in the absence and presence of DNA respectively; K_b, the binding constant; n, the number of binding sites on DNA; and [DNA] the concentration of DNA solution. Plots of $\log[(F_0–F)/F]$ against log [DNA] would provide the values of n (from the slope)and K_b (from the intercept). The experiments were repeated three times and standard deviations were given in Table 2.

Determination of binding 3Q to BSA using fluorescence measurements

The binding of water soluble complex **3Q** to BSA were studied by spectrofluorometry at room temperature. An aqueous solution of **3Q** (10.0 µM, 2.5 mL) was titrated by successive additions of 10.0 µL aliquots of 20.0 µM BSA. After each addition of BSA, the fluorescence emission spectra were recorded. The concentration of BSA along the titration varied from 0 to 0.47 µM. Fluorescence excitation and emission spectra were obtained from solutions of BSA and quaternized zinc Pc (**3Q**) were prepared in distilled water. Excitation and emission slits were set at 10 nm bandpass at 900 V. Pcs solutions were excited at 655 nm and spectra were recorded between 650 and 850 nm. The steady diminution in Pcs fluorescence with increase in BSA concentrations was noted and used in the determination of the binding constants and the number of binding sites on DNA, according to Eq. (4) [44]. All K_b constants for BSA were calculated by the same methods and the same mathematical equations (2-4) used in DNA measurements. The experiments were repeated three times and standard deviations were given in Table 2.

Determination of quenching effect of 3Q on the fluorescence intensity of DNA–SYBR complex by using Ksv constants

In order to determine the binding mode of **3Q** to DNA, the decrease in emission of DNA-SYBR complex around 530 nm was monitored indicating the competitive binding of SYBR with quaternized Pcs **3Q**. The concentration of the purchased SYBR Gold was 10000X and was diluted to 1X. Each of six fluorescence cuvettes contained the solution of SYBR at a fixed concentration of 1X (200.0 µL) and the solution of DNA (50.0 µM, 1.8 mL). At a final concentration of 0, 0.91, 1.66, 2.30, 2.85 and 3.33 µM, 200 µL solutions of quaternized Pc **3Q** was added to the solution of SYBR–DNA complex in each cuvette. The samples were excited at 497 nm and the spectra were recorded from 520 to 650 nm consecutively at 900 V with a slit of 10 nm for both excitation and emission. All solutions were prepared in distilled water. The quenching effect of quaternized Pc **3Q** on the fluorescenceof SYBR–DNA complex

was calculated by using Stern–Volmer relationship [46] according to Eq. (5):

$$F_0/F = K_{sv}[Pc] + 1 \quad (5)$$

where F_0 and F are the fluorescence intensities of the excited DNA–SYBR complex in the absence and presence of Pcs, [Pc] is the concentration of **3Q** and K_{SV} is the Stern–Volmer constant. The slope of the plots of F_0/F versus [Pc] provide the value of Ksv which indicates the affinity of quaternized Pcs **3Q** to DNA. The measurements were repeated three times and standard deviations were calculated.

Determination of quenching effect of 3Q on the fluorescence intensity of BSA-AO complex by using Ksv constants

In order to determine the binding mode of **3Q** to BSA, the decrease in emission of BSA-AO complex around 350 nm was monitored indicating the competitive binding of AO with quaternized Pcs **3Q**. The concentration of the purchased AO was 20.0 μM. Each of ten fluorescence cuvettes contained the solution of AO (20.0 μM, 200 μL) and the solution of BSA (50 μM, 1.8 mL). At a final concentration varied from 0 to 2.60 μM, 30 μL solutions of quaternized Pc **3Q** was added to the solution of BSA-AO complex in each cuvette. The samples were excited at 280 nm and the spectra were recorded from 300 to 500 nm consecutively at 900 V with a slit of 10 nm for both excitation and emission. All solutions were prepared in distilled water. All K_{sv} constants for BSA were calculated by the same methods and the same mathematical equations (2-5) used in DNA measurements. The measurements were repeated three times, standard deviations were calculated and given in paranthesis.

Acknowledgements

This work was supported by Research Fund of the Istanbul Technical University and TUBITAK (Project no: 109T163).

Notes and references

1. D. Dini and M. Hanack, in *The Porphyrin Handbook*, eds. K. Kadish, R. Guilard and K. M. Smith, Academic Press, 2003, vol. 15, ch. 107, pp. 1-36.
2. E. Benhur and I. Rosenthal, *Int. J. Radiat. Biol.*, 1985, 47, 145-147.
3. F. Dumoulin, M. Durmus, V. Ahsen and T. Nyokong, *Coord. Chem. Rev.*, 2010, 254, 2792-2847.
4. M. Durmus and V. Ahsen, *J. Inorg. Biochem.*, 2010, 104, 297-309.
5. B. S. Sesalan, A. Koca and A. Gul, *Dyes Pigment.*, 2008, 79, 259-264.
6. C. Uslan, K. T. Oppelt, L. M. Reith, B. S. Sesalan and G. Knor, *Chem. Commun.*, 2013, 49, 8108-8110.
7. D. C. Carter and J. X. Ho, *Adv.Protein Chem.*, 1994, 45, 153-203.
8. U. Kraghhansen, *Pharmacol. Rev.*, 1981, 33, 17-53.
9. T. Tanaka, S. Shiramoto, M. Miyashita, Y. Fujishima and Y. Kaneo, *Int. J. Pharm.*, 2004, 277, 39-61.
10. J. P. Taquet, C. Frochot, V. Manneville and M. Barberi-Heyob, *Curr. Med. Chem.*, 2007, 14, 1673-1687.
11. A. M. Zhang, J. Huang, X. C. Weng, J. X. Li, L. G. Ren, Z. B. Song, X. Q. Xiong, X. Zhou, X. P. Cao and Y. Zhou, *Chem. Biodivers.*, 2007, 4, 215-223.
12. O. L. Kaliya, E. A. Lukyanets and G. N. Vorozhtsov, *J. Porphyr. Phthalocyanines*, 1999, 3, 592-610.
13. D. Demirkapi, A. Sirin, B. Turanli-Yildiz, Z. P. Cakar and B. S. Sesalan, *Synth. Met.*, 2014, 187, 152-159.
14. D. Evren, A. K. Burat, I. Ozcesmeci and B. S. Sesalan, *Dyes Pigment.*, 2013, 96, 475-482.
15. D. Evren, I. Ozcesmeci, B. S. Sesalan and A. K. Burat, *Synth. Met.*, 2013, 168, 31-35.
16. B. Turanli-Yildiz, T. Sezgin, Z. P. Cakar, C. Uslan, B. S. Sesalan and A. Gul, *Synth. Met.*, 2011, 161, 1720-1724.
17. C. Uslan and B. S. Sesalan, *Inorg. Chim. Acta*, 2013, 394, 353-362.
18. S. Y. Al-Raqa, *Dyes Pigment.*, 2008, 77, 259-265.
19. J. P. Fox and D. P. Goldberg, *Inorg. Chem.*, 2003, 42, 8181-8191.
20. J. H. Wang, A. K. Khanamiryan and C. C. Leznoff, *J. Porphyr. Phthalocyanines*, 2004, 8, 1293-1299.
21. A. Atsay, A. Gul and M. B. Kocak, *Dyes Pigment.*, 2014, 100, 177-183.
22. O. Kurt, I. Ozcesmeci, A. Gul and M. B. Kocak, *J. Organomet. Chem.*, 2014, 754, 8-15.
23. E. Guzel, A. Atsay, S. Nalbantoglu, N. Saki, A. L. Dogan, A. Gul and M. B. Kocak, *Dyes Pigment.*, 2013, 97, 238-243.
24. A. Lyubimtsev, Z. Iqbal, G. Crucius, S. Syrbu, E. S. Taraymovich, T. Ziegler and M. Hanack, *J. Porphyr. Phthalocyanines*, 2011, 15, 39-46.
25. Z. Biyiklioglu, M. Durmus and H. Kantekin, *J. Photochem. Photobiol. A-Chem.*, 2010, 211, 32-41.
26. G. Barbieri, R. Benassi, P. Lazzeretti, L. Schenetti and F. Taddei, *Organic Magnetic Resonance*, 1975, 7, 451-454.
27. N. B. McKeown, H. Li and M. Helliwell, *J. Porphyr. Phthalocyanines*, 2005, 9, 841-845.
28. K. Kasuga, K. Yashiki, T. Sugimori and M. Handa, *J. Porphyr. Phthalocyanines*, 2005, 9, 646-650.
29. M. J. Stillman and T. Nyokong, *Phthalocyanines : properties and applications*, VCH, New York, NY, 1989.
30. H. R. P. Karaoglu, A. Koca and M. B. Kocak, *Dyes Pigment.*, 2012, 92, 1005-1017.
31. I. Ozcesmeci, *Synth. Met.*, 2013, 176, 128-133.
32. A. Ogunsipe and T. Nyokong, *J. Photochem. Photobiol. A-Chem.*, 2005, 173, 211-220.
33. M. Canlica and T. Nyokong, *Polyhedron*, 2011, 30, 1975-1981.
34. E. T. Saka, M. Durmus and H. Kantekin, *J. Organomet. Chem.*, 2011, 696, 913-924.
35. S. I. Pillai, K. Vijayaraghavan and S. Subramanian, *Der Pharma Chemica*, 2014, 6, 379-389.
36. D. Agudelo, P. Bourassa, G. Berube and H. A. Tajmir-Riahi, *Int. J. Biol. Macromol.*, 2014, 66, 144-150.
37. S. Nafisi, A. A. Saboury, N. Keramat, J. F. Neault and H. A. Tajmir-Riahi, *J. Mol. Struct.*, 2007, 827, 35-43.
38. G. Cosa, K. S. Focsaneanu, J. R. N. McLean, J. P. McNamee and J. C. Scaiano, *Photochem. Photobiol.*, 2001, 73, 585-599.
39. K. R. Fox, *Drug-DNA Interaction Protocols*, Humana Press, New Jersey, 1997.
40. A. Ogunsipe and T. Nyokong, *Photochem. Photobiol. Sci.*, 2005, 4, 510-516.
41. R. Itri, W. Caetano, L. R. S. Barbosa and M. S. Baptista, *Braz. J. Phys.*, 2004, 34, 58-63.
42. X. Z. Feng, Z. Lin, L. J. Yang, C. Wang and C. L. Bai, *Talanta*, 1998, 47, 1223-1229.
43. D. D. Perrin and W. L. F. Armarego, *Purification of Laboratory Chemicals*, Pergamon, Oxford, Second edition edn., 1989.
44. W. B. A. Duan, Z. X. Wang and M. J. Cook, *J. Porphyr. Phthalocyanines*, 2009, 13, 1255-1261.
45. E. Lissi, C. Calderon and A. Campos, *Photochem. Photobiol.*, 2013, 89, 1413-1416.
46. D. Cakir, V. Cakir, Z. Biyiklioglu, M. Durmus and H. Kantekin, *J. Organomet. Chem.*, 2013, 745, 423-431.